Kramers-Moyal coefficients in the analysis and modeling of heart rate variability

M. Petelczyc* and J. J. Żebrowski†
Faculty of Physics, Warsaw University of Technology, Koszykowa 75,00–662 Warsaw, Poland

R. Baranowski‡
National Institute of Cardiology, Alpejska 42, 04–628 Warsaw, Poland

(Received 8 February 2009; revised manuscript received 25 May 2009; published 18 September 2009)

Modeling of recorded time series may be used as a method of analysis for heart rate variability studies. In particular, the extraction of the first two Kramers-Moyal coefficients has been used in this context. Recently, the method was applied to a wide range of signal analysis: from financial data to physiological and biological time series. Modeling of the signal is important for the prediction and interpretation of the dynamics underlying the process. The method requires the determination of the Markov time. Obtaining the drift and diffusion term of the Kramers-Moyal expansion is crucial for the modeling of the original time series with the Langevin equation. Both Tabar *et al.* [Comput. Sci. Eng. **8**, 54 (2006)] and T. Kuusela [Phys. Rev. E **69**, 031916 (2004)] suggested that these terms may be used to distinguish healthy subjects from those with heart failure. The research groups applied a somewhat different methodology and obtained substantially different ranges of the Markov time. We show that the two studies may be considered consistent with each other as Kuusela analyzed 24 h recordings while Tabar *et al.* analyzed daytime and nighttime recordings, separately. However, both groups suggested using the Langevin equation for modeling of time series which requires the fluctuation force to be a Gaussian. We analyzed heart rate variability recordings for ten young male (age $26-4+3$ y) healthy subjects. 24 h recordings were analyzed and 6-h-long daytime and nighttime fragments were selected. Similar properties of the data were observed in all recordings but all the nighttime data and seven of the ten 24 h series exhibited higher-order, non-negligible Kramers-Moyal coefficients. In such a case, the reconstruction of the time series using the Langevin equation is impossible. The non-negligible higher-order coefficients are due to autocorrelation in the data. This effect may be interpreted as a result of a physiological phenomenon (especially occurring for nighttime data): respiratory sinus arrhythmia (RSA). We detrended the nighttime recordings for the healthy subjects and obtained an asymmetry in the dependence of the diffusion term on the rescaled heart rate. This asymmetry seems to be an effect of different time scales during the inspiration and the expiration phase of breathing. The asymmetry was significantly decreased in the diffusion term found for detrended nighttime recordings obtained from five hypertrophic cardiomyopathy (HCM) patients. We conclude that the effect of RSA is decreased in the heart rate variability of HCM patients—a result which may contribute to a better medical diagnosis by supplying a new quantitative measure of RSA.

DOI: 10.1103/PhysRevE.80.031127 PACS number(s): 02.50.Fz, 02.50.Ga, 05.10.Gg

I. INTRODUCTION

Recently, the extraction of the first two Kramers-Moyal coefficients was applied to financial data [1–3]. The data were assumed to be stationary. Linear trends were removed by using in the calculation relative changes of the time series: increments of returns, logarithmic returns, and absolute changes (increments). However, financial time series are known to have fat-tailed distributions especially in small time scales: the probability density of large fluctuations is high [4]. In spite of this, the data were analyzed using the Langevin equation. The switching time in ion transport through biochannels shows similar properties: a power-law distribution for the channel closed times [5,6]. In this research, negligible higher-order Kramers-Moyal coefficients were obtained for the time series analyzed. However, the occurrence of higher Kramers-Moyal terms should be expected for a non-Gaussian fluctuation force.

In the literature, one may find examples of data with nonvanishing higher-order Kramers-Moyal coefficients: the Dow-Jones index (DJI) fluctuations [3] and the motion of the Rayleigh particle. Lim *et al.* [3] suggested that nonvanishing fourth-order coefficient for DJI is due to nonstationarity. Plyukhin [7] showed that the results obtained depend on the assumptions about the damping force acting on a massive particle: the higher corrections in Fokker-Planck equation were found to be important when the random force is not Gaussian distributed. It can be seen that the problem of the occurrence of the higher-order Kramers-Moyal coefficients is complex and crucial not only for the reconstruction of the data by means of a stochastic equation but also for the description of the process.

In this paper, we focus on the analysis of heart rate variability data in the form of time series of intervals between heart beats (the distance in time between consecutive R waves-the RR interval of the electrocardiogram trace). Recently, the reconstruction of the Langevin equation had been also applied to the analysis of RR interval time series [8–10]. The drift and diffusion coefficients of the Kramers-Moyal expansion were extracted from measured data. This seems to be a very promising way of modeling heart rate variability.

*petelczyc_m@if.pw.edu.pl
†zebra@if.pw.edu.pl
‡rbaranowski@ikard.pl

The results published so far show important differences in the functional dependence of the drift term on the rescaled magnitude of the RR interval between healthy subjects and congestive heart failure patients [9]. The method may potentially be used as a diagnostic tool. The functional forms of the first two coefficients of the Kramers-Moyal expansion should be useful for the physiological interpretation of heart rate variability. The drift term describes the deterministic properties of the process, while the diffusion term is the amplitude of the random term of the Langevin equation. The latter term may yield information on the properties of random forces acting on the system. In addition, the knowledge of their functional dependence may allow the reconstruction of the signal with similar properties as the original data and so the understanding of its nature.

The description of heart rate variability with the use of the Kramers-Moyal expansion seems not complete and the stochastic properties are not fully understood. The aim of this study is to analyze the properties of the drift and diffusion terms and their relation to oscillations in the human cardiovascular system. We also compute four higher-order coefficients of the Kramers-Moyal expansion and discuss their magnitude. We show that detrended nighttime series analysis reveals an asymmetry in the diffusion term for normal subjects which may be interpreted as the occurrence of two different time scales in the respiration process. While both Kuusela [8] and Tabar *et al.* [9] analyzed only the first two terms of the expansion (i.e., the drift and diffusion coefficients), we obtain non-negligible higher-order terms of Kramers-Moyal expansion for the nighttime data of the healthy subjects and mostly for 24 h series. In that case, those signals, for which higher nonvanishing terms are given, cannot be reconstructed using the Langevin equation. We check whether nonstationarity in the data can be the reason for the occurrence of non-negligible higher Kramers-Moyal coefficients. After removing the linear trends from the data recorded during the nighttime, we still obtain the higher-order terms in the expansion. The occurrence of higher-order expansion terms may be interpreted: it is the effect of respiratory sinus arrhythmia (RSA)—a physiological phenomenon and an important source of heart rate variability. We show that the asymmetry in the functional properties of the diffusion term is impaired or does not occur for hypertrophic cardiomyopathy patients—a result which may in the future enhance medical diagnosis of this disease.

II. KRAMERS-MOYAL EXPANSION

Given the time series $X(t)$, the coefficients $D^{(n)}(X,t)$ of the Kramers-Moyal expansion [11] need to be determined

$$\frac{\partial P(X,t)}{\partial t} = \sum_{n=1} \left(-\frac{\partial}{\partial X} \right)^n D^{(n)}(X,t) P(X,t), \tag{1}$$

$$D^{(n)}(X,t) = \frac{1}{n!} \lim_{\tau \to 0} \frac{1}{\tau} \langle [X(t+\tau) - X(t)]^{(n)} \rangle, \tag{2}$$

where $\tau > 0$ and $P(X,t)$ denotes the probability density of obtaining X at time t. The Markov time τ may be evaluated from the Chapman-Kolmogorov (CK) equation, which Markov processes obey:

$$P(X_2, t+\tau | X_1, t-\tau) = \int P(X_2, t+\tau | X_3, t) P(X_3, t | X_1, t-\tau) dX_3, \tag{3}$$

with X_1, X_3, X_2 at the given points in time $t_1 = t-\tau$, $t_3 = t$, $t_2 = t+\tau$, respectively. $P(X_i, t_i | X_k, t_k)$ is the conditional probability density. In Eq. (3), the time interval between X_1, X_3, and X_2 is taken to be equal, which means that our process is assumed to be stationary [12].

From the Pawula theorem [11], it follows that, when $D^{(n)}(X,t) = 0$ for $n \geq 3$, Eq. (1) may be rewritten as the Fokker-Planck equation with the drift ($D^{(1)}$) and diffusion ($D^{(2)}$) terms

$$\frac{\partial P(X,t)}{\partial t} = -\frac{\partial}{\partial X} D^{(1)}(X,t) P(X,t) + \frac{\partial^2}{\partial X^2} D^{(2)}(X,t) P(X,t). \tag{4}$$

If the assumptions of the Pawula theorem hold, Eq. (4) is equivalent to the Langevin equation, which describes the dynamics of the process

$$\frac{dX}{dt} = D^{(1)}(X,t) + \sqrt{2D^{(2)}(X,t)}\Gamma(t), \tag{5}$$

where $\Gamma(t)$ is Gaussian noise with $\langle \Gamma(t) \rangle = 0$ and $\langle \Gamma(t)\Gamma(t') \rangle = \delta(t-t')$. As the process is stationary, the drift and diffusion coefficients are functions of X and not the time variable but of a constant—the Markov time.

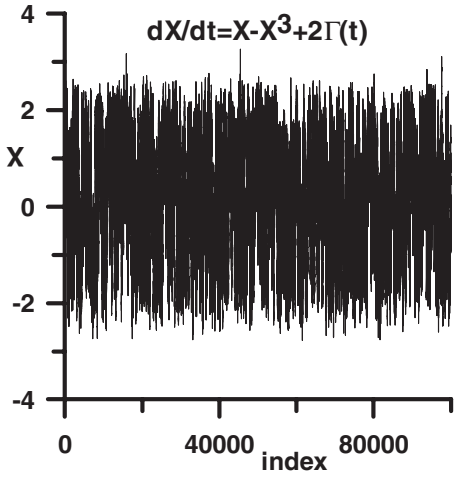

FIG. 1. Time series generated using a third-order deterministic potential and an additive Gaussian noise (with zero mean and standard deviation equal to unity).

III. TEST OF THE METHOD

We generated a process with a cubic nonlinearity and an additive Gaussian noise $\Gamma(t)$ with a zero mean and the standard deviation equal to unity (Fig. 1) using the equation

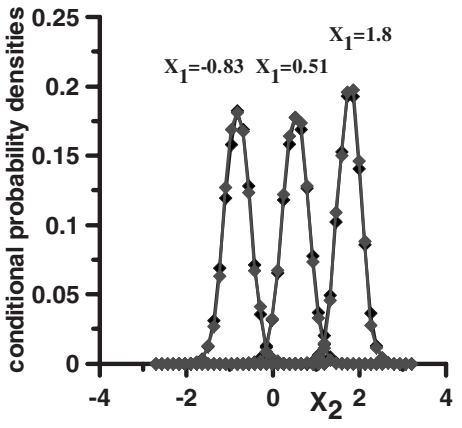

FIG. 2. Conditional probability densities of the CK test for the data presented in Fig. 1. Black curves correspond to the left side of Eq. (3) and gray correspond to the right side of the Eq. (3), respectively.

$$\frac{dX}{dt} = X - X^3 + 2\Gamma(t). \tag{6}$$

Equation (6) was integrated numerically using the method described in Ref. [13] with a time step of 0.01 and the initial condition $X_0=0.1$. We generated 10^5 points. The Markov time was determined using the CK test Eq. (3). For computational analysis, Eqs. (2) and (3) were discretized by dividing the range of X into a constant number of 45 bins. We used the formula $R=\frac{\Sigma_{i=1}y_i^2-\Sigma_{i=1}[y_i-f(x_i)]^2}{\Sigma_{i=1}y_i^2}$ to estimate the quality of the fit in the CK test. In Fig. 2, it can be seen that the fit was very good with $R=0.99$. Next, we calculated the first six coefficients of the Kramers-Moyal expansion. The drift and diffusion terms are presented in Figs. 3(a) and 3(b) (black points) as functions of X. From the Langevin equation (5) and from the equation for the generated process Eq. (6), we expected the drift term to be a cubic function and the diffusion term—a constant. To find the constant value for $D^{(2)}$, we looked for such a range of X for which the linear fit had the

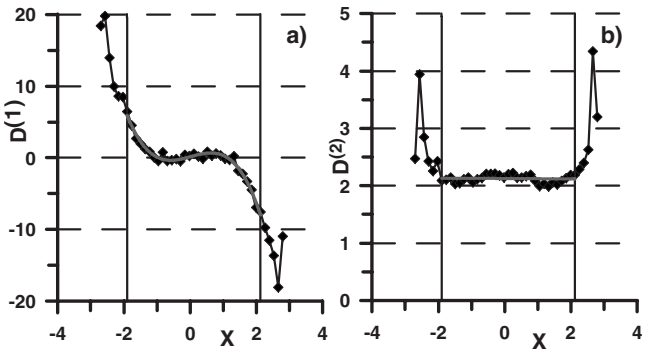

FIG. 3. (a) Drift term (diamond symbols) with the range of the variable X, for which the cubic fit (gray line) quality of estimation coefficient is $R=0.98$, marked by the solid vertical lines. The solid line passing through the diamonds is for the convenience of the eyes only. (b) Diffusion term (diamond symbols) with the range of X values, for which the average of $D^{(2)}$ was equal to 2.13, marked by vertical lines. The gray horizontal line marks the average value.

smallest directional coefficient. The best fit range is marked in Figs. 3(a) and 3(b) by thin vertical lines. In this range, the function $ax-bx^3$ was fit to $D^{(1)}$ [Fig. 3(a)] with $a=b=1.0$ and the Pearson correlation coefficient was $R=0.98$. The average value of $D^{(2)}$ is equal 2.13 for this range. We thus obtained an acceptable agreement between the properties of the model and the coefficients extracted from the time series generated by the model.

The higher-order terms of the expansion had negligible values (not shown). For example, $D^{(3)}$ was over 1 order of magnitude smaller than $D^{(1)}$ and $D^{(4)}$ was even 2 orders of magnitude smaller than $D^{(2)}$. According to the Pawula theorem, when the higher-order coefficients vanish, the process can be described by the Langevin equation (5). Thus, assuming that at least a 1 order of magnitude difference between the corresponding successive odd (and even, respectively) coefficients is sufficient, the dynamics underlying the test process can be considered known and it is possible to reconstruct it using the Langevin equation.

IV. MEDICAL DATA AND SIGNAL ANALYSIS

Heart rate variability data were extracted during routine medical examinations from 24 h Holter ECG recordings using the 563 Strata Scan Del Mar Avionics system at the Institute of Cardiology (Warszawa, Poland). All data were checked by a qualified cardiologist: normal beats were detected, artifacts were deleted by hand, and arrhythmias were recognized. The data were sampled at 128 Hz.

Heart rate variability for ten young (age 26−4+3 y) healthy males was analyzed. Five data sets for hypertrophic cardiomyopathy (HCM) were also analyzed (2 men and 3 women 26.5+/−2 y). HCM is generally a pathology of the heart cells but abnormalities in the autonomic regulation are also observed in this disease so that its progress may affect heart rate variability.

From the 24 h recordings for the normal subjects, we extracted 6 h daytime (between 10.30 a.m. and 8 p.m.) and nighttime (between 10.30 p.m. and 6 a.m.) fragments. From 24 h HCM recordings, 6 h nighttime data were selected: we chose such fragments of the recording which were recorded at least 1.5 h after the Holter was switched on and contained as little as possible of periods with a linear trend. We checked that, during the night hours, the averages of RR intervals were all above 900 ms (but do not exceed 1300 ms). In selecting the nighttime recordings, we chose such fragments of the recordings for which the average RR interval was at least 900 ms.

A detrending method [14] was used in one of the sections below. The signal was smoothed by a 100-data-point sliding window. The extrema of the smoothed signal were determined. Linear trends were found between successive extrema and removed from data. Finally, the resultant signal was rescaled to regain the original range of the data.

V. COMPARISON OF 24 H RECORDINGS WITH THE 6 H FRAGMENTS

Heart rate variability data differ from subject to subject. For comparison, all recordings were rescaled taking into ac-

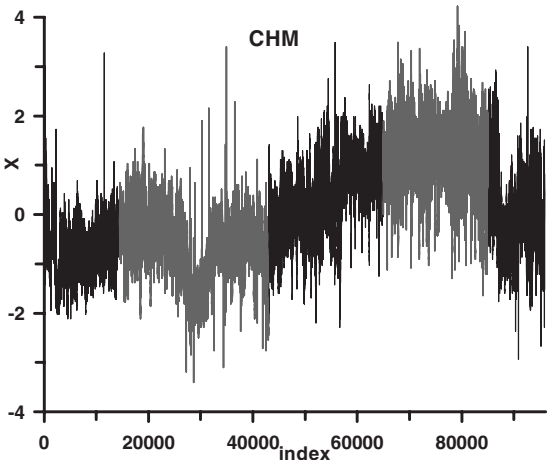

FIG. 4. The 24 h rescaled RR intervals time series for a healthy subject (CHM). The left fragment in gray is the 6 h daytime data; the right one is the 6 h nighttime fragment used in the analysis.

count the mean value $\langle RR \rangle$ and standard deviation σ of the 24 h signal: $X_i = \frac{RR_i - \langle RR \rangle}{\sigma}$ (Fig. 4 with the daytime and nighttime segments of the data marked in gray). For the healthy subjects, the Markov time τ for the 24 h recordings, the day and the nighttime fragments varied between 1 and 4, measured in values of the RR interval index. Using the estimated τ, we calculated the first six Kramers-Moyal coefficients.

Because of the low number of the very short and the very long RR intervals in all data series, the errors of the Kramers-Moyal terms for extreme values of the argument can be large due to the poor statistics at the extreme ends of the RR intervals distribution. The recognition of this effect is crucial for the proper measurement of the expansion coefficients. In most of the analysis of the medical data, we decided to limit the range of X to such for which the statistics is satisfactory, i.e., the number of data points in a given bin exceeds 10^2. In Figs. 5–8, we depicted the expansion coefficients for the complete range of the X variable only for three healthy persons (a signal with small 24 h standard deviation—patient LAS, with a medium one—patient KWL, and with a large one—patient BDR). In addition, in these figures, we marked by thin, vertical lines the range of satisfactory statistics which was obtained for a single, chosen case (KWL). The correct range for the other cases did not differ significantly.

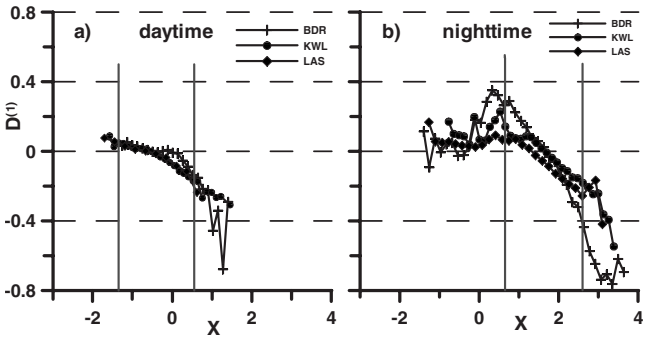

FIG. 6. Drift terms (a) for daytime signals with one, two, or three zeros and (b) for three nighttime signals with a single zero—within the good statistics range. The acronyms denote the individual recordings. Gray vertical lines mark the good statistics range for the subject KWL.

The drift term for all 24 h recordings studied had three or more zeros (Fig. 5). Similar results were obtained in Refs. [9,10]. We found that, within the daytime segments, the drift term had one, two, or three zeros [Fig. 6(a)], while within the nighttime recordings, only one [Fig. 6(b)]. In two cases, for the nighttime series, more zeros were obtained (for subject BDR, five zeros and for KWR, three zeros), but within the range of good statistics, only a single case (KWR) had three zeros. The presence of additional zeros can be explained by nonstationarity, when trends or abrupt changes of the mean value affect the calculation [10].

The diffusion term $D^{(2)}$ for the 24 h recordings had at least a single local minimum (Fig. 7), similar to the results of Kuusela [8]. Moreover, for the 6 h fragments, especially for the nighttime data, we obtained a single local minimum in $D^{(2)}$ (Figs. 8(a) and 8(b)]. In most cases, we can see fluctuations in the drift and diffusion terms for the extreme values of X which—as in the case of the test signal—are due to poor

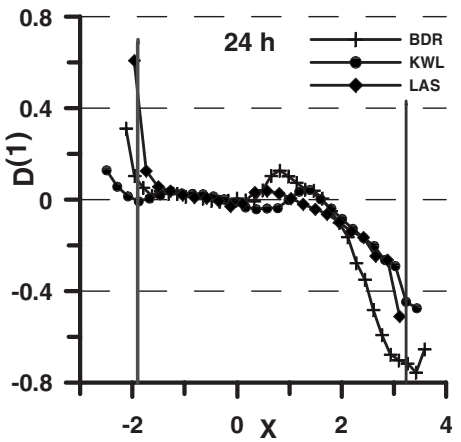

FIG. 5. Drift terms for 24 h time series usually exhibit three zeroes. The acronyms denote individual recordings. Gray vertical lines mark the good statistics range for the subject KWL.

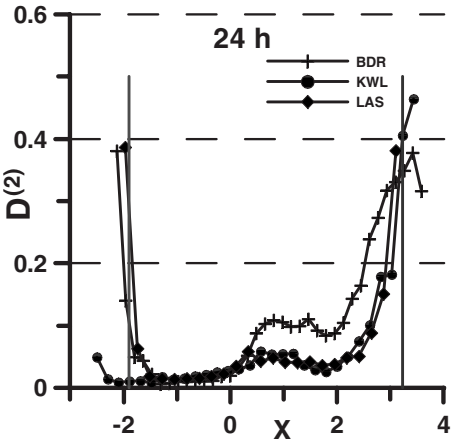

FIG. 7. Diffusion terms for the 24 h time series. Note the local minima. The acronyms denote the individual recordings. Gray vertical lines mark the good statistics range for the subject KWL.

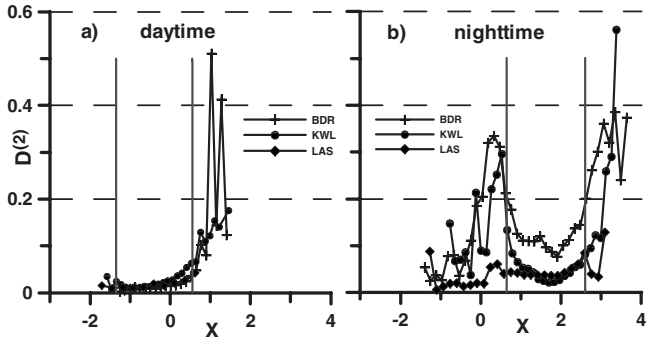

FIG. 8. Diffusion terms for (a) the daytime fragments and (b) the nighttime fragments. Note the well-visible local minimum or minima for each curve. The acronyms denote the individual recordings. Gray vertical lines mark the good statistics range the subject KWL.

statistics in these ranges of X. In the finite range of X between these extremes, especially for the nighttime recordings, we can fit a linear or a parabolic function (for $D^{(1)}$) and a second- or fourth-order polynomial (for $D^{(2)}$). The functional dependences of the results for daytime are more complicated due to trends in the data. We believe that the night fragments are better to study because they include less factors such as stress, physical effort, etc., the presence of which destroys stationarity. It is well known that—quite apart from nonstationarity—the heart rate variabilities during the day and during the night differ. In particular, the average heart rate is different [15], the variance is larger during the night [16,17], while the LF and HF contents in the power spectrum are different [15]. It has been shown also that some statistical properties are different [18].

The Markov time evaluated from the 24 h recordings was applied to the nighttime and the daytime segments and we found a good agreement. In Figs. 9(a) and 9(b), it can be seen that the diffusion and the drift terms from the day and nighttime data for the normal GRG are parallel or overlap specific segments of the 24 h recordings. We obtained the same result for all other cases studied here. This shows that the functions of drift and diffusion obtained by Tabar [9] are comparable to those obtained by Kuusela [8] except that data from different times of the day were used in the former of the two studies.

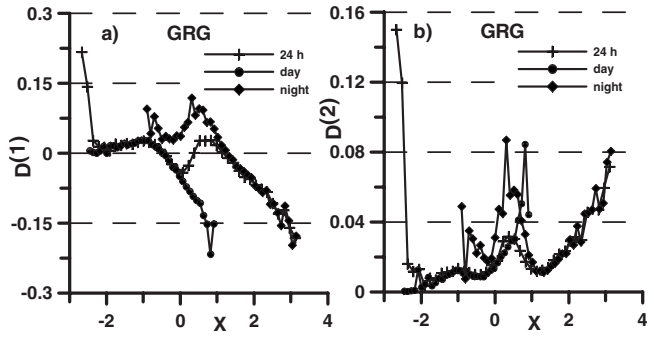

FIG. 9. (a) Daytime and nighttime drift terms overlap the corresponding parts of the curve obtained for the 24 h signal. (b) The minima of the daytime and nighttime diffusion terms overlap with the minima in the 24 h signal.

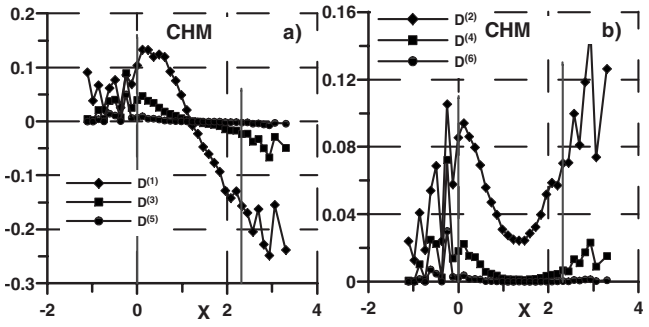

FIG. 10. (a) Odd higher-order Kramers-Moyal coefficients and (b) even higher-order Kramers-Moyal coefficients for the nighttime signal for a single healthy subject. Gray vertical lines marked the good statistics range.

VI. HIGHER-ORDER EXPANSION COEFFICIENTS

Besides the drift and diffusion coefficients, we calculated four higher-order Kramers-Moyal coefficients. For the daytime fragments, their values were found to be negligible. The magnitudes of the higher-order terms for the nighttime series (especially for $D^{(3)}$ and $D^{(4)}$) are non-negligible compared to $D^{(1)}$ and $D^{(2)}$ in most cases. Figure 10(a) depicts the first three odd-order coefficients while Fig. 10(b) the even-order coefficients for the case CHM, a typical example. In the range of X-yielding acceptable statistics marked with vertical lines, the $D^{(3)}$ and $D^{(4)}$ attain more than 10% of $D^{(1)}$ and $D^{(2)}$, respectively. This happens also for the extreme values of X, but usually the coefficients obtained in these ranges of the argument should not be taken into account because of the statistical errors. For seven of the ten 24 h recordings, we also observed higher-order nonvanishing Kramers-Moyal terms. Because the nighttime and daytime fragments were extracted from the 24 h recordings, the properties of the shorter time series may be found in the 24 h data. Moreover, a process, which is dominant in the night, may occur in a wider range of the time than the 6 h selected for analysis. Note that 24 h signals include additional, external factors which lead to nonstationarity. We see then that the Langevin equation, in general, may not be used to describe the dynamics of nighttime heart rate variability data.

VII. DETRENDING THE SIGNAL

To check whether the occurrence of the higher-order terms in the Kramers-Moyal expansion of the nighttime data is not due to nonstationarity, we applied the above-described detrending method to our data. Figure 11 depicts an example of the effect of our method on the data. The gray curve (left axis in Fig. 11) depicts the original data while the black one the same data but detrended (right axis). Note that a by-product of the detrending method is a symmetrization of the data. However, contrary to the suggestion in Lim *et al.* [3], after detrending, we still obtain the higher-order non-negligible Kramers-Moyal coefficients. In fact, the higher-order terms remain the same after detrending, except for extreme ranges of X, for which we observed even a 1 order increase.

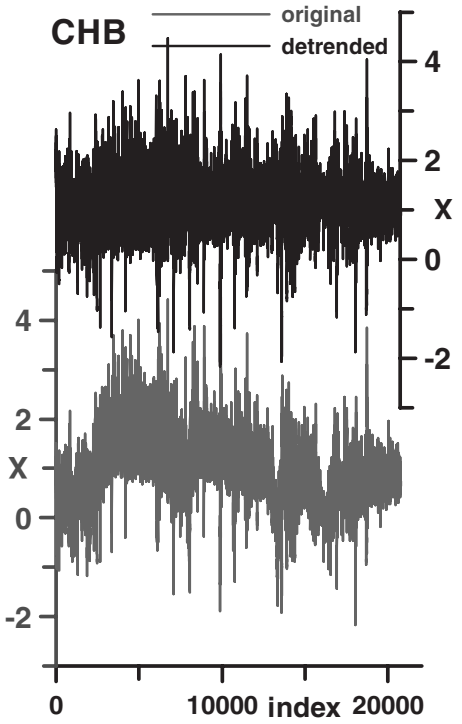

FIG. 11. The original (gray) and detrended (black) nighttime recordings for the subject CHB.

Removing trends from the data, we obtained a different functional dependence for the drift and diffusion terms. Figures 12(a) and 12(b) depict an example of the functional dependence of $D^{(1)}$ and $D^{(2)}$ on X for the case CHB with the coefficients obtained from the detrended data marked in black and those from the original data in gray. In Figs. 12(a) and 12(b), we marked the range of good statistics (i.e., with more than 10^2 points per bin) for the detrended data with black vertical lines. It can be seen that $D^{(1)}$ became a linear function for a wider range of arguments, while $D^{(2)}$ became an asymmetrical function. In Fig. 12(b), it can also be seen that the detrending leaves the $D^{(2)}$ curve to the right of the minimum practically unchanged. However, to the left of this

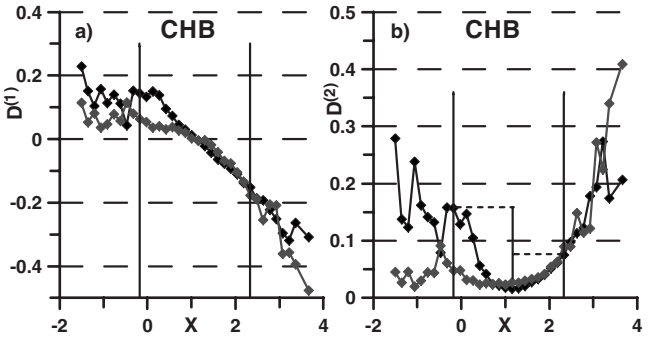

FIG. 12. (a) Drift term for original (gray) and detrended (black) nighttime recordings for subject CHB. (b) Diffusion term for the original (gray) and detrended (black) nighttime recordings for subject CHB. The horizontal black dashed lines show the asymmetry between left and right parts of diffusion curve for detrended data. Gray vertical lines marked the good statistics range for detrended data.

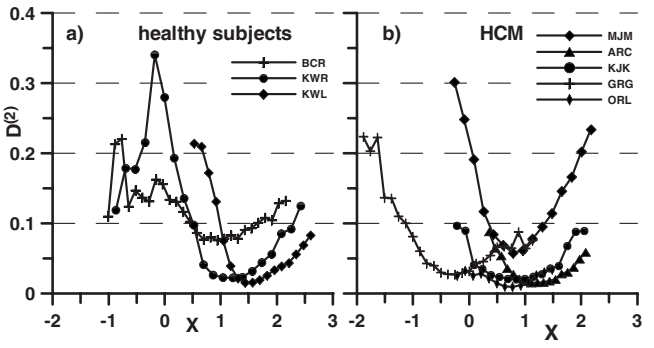

FIG. 13. Diffusion terms for (a) the detrended nighttime signals for three healthy subjects and (b) detrended nighttime signals for five HCM patients. All diffusion terms are shown within the range of good statistics only.

point, the curve increases faster than that for the original data (in Fig. 12(b): the horizontal black dashed lines show the asymmetry between the left and the right part of diffusion curve for the detrended data). In Fig. 13(a), we present the diffusion term for three detrended nighttime recordings showing only the points calculated within the good statistics range. For a single case, STR (not shown), we did not obtain an asymmetrical $D^{(2)}$ curve.

Note that for three of the original—not detrended—nighttime series, for which the drift is a linear function, the diffusion term also has a characteristic asymmetry. This may indicate that these cases were less nonstationary than the others. A linear dependence of the drift coefficient was recently obtained in Refs. [9,10], but the properties of the functional form of $D^{(2)}$ (except the estimation of a functional dependence) were not studied in detail.

VIII. RSA IN NIGHTTIME RR INTERVAL SERIES

To the right of $X=0$, the flatter part of the $D^{(2)}$ curve corresponds to long RR intervals, which may suggest a correlation with the deceleration capacity (DC) [19] of the heart rate. Consequently, the diffusion term for the range of X to the left of zero may be interpreted as a measure of the acceleration capacity (AC). The asymmetry in the diffusion term is related to the different time scales of the acceleration and deceleration of heart rate. The capacities DC and AC provide information about both the vagal and sympathetic activities as well as the related oscillations (such as respiration) and baroreflex activity [19]. The non-negligible higher-order coefficients and the linear dependence for the drift may indicate an oscillating process in the nighttime data which induces an increased correlation. A good candidate for such an oscillation, and well known to dominate during the night, is RSA [19,20] which is dominant mostly for children and the young [21] but occurs in a weaker form in adults. The asymmetry in the functional dependence of the diffusion term is a consequence of the asymmetry during the inspiration and expiration phases of RSA. Respiratory sinus arrhythmia is itself easy to detect. However, there seem to be no good ways of a quantitative assessment of this phenomenon. It is, however, one of the reasons for heart rate variability: the RR interval

shortens during the inspiration phase of breathing and it is lengthened during expiration. The nighttime recordings appear to be best for studies of the properties of RSA because the external factors act less so that the dominant oscillations in the heart rate seem to be mainly due to RSA.

If the heart loses its capacity for acceleration or deceleration, heart rate variability decreases. This usually happens in pathology. As an example, we present the diffusion terms within the good statistics range [Fig. 13(b)] obtained for detrended nighttime recordings of heart rate variability for five cases of hypertrophic cardiomyopathy. Note that the minima of $D^{(2)}$ do not coincide because average and standard deviation of 24 h signal differ for each case. In comparison to the results for the healthy subjects [Fig. 13(a)], the asymmetry of $D^{(2)}$ was not obtained in three of the five subjects studied (the exceptions were GRD and MJM). Since the occurrence of the asymmetry seems to be typical for healthy subjects, the lack of asymmetry (or a weakening of asymmetry) in the functional form of $D^{(2)}$ may be taken as a measure of the level of pathology. However, to show this fully, a much larger group of patients needs to be studied.

IX. SUMMARY

The method of extraction of the Kramers-Moyal coefficients was implemented and tested using an artificial time series and the correct data range yielding satisfactory statistics determined. We applied the method to analyze heart rate variability. Our research repeats parts of the recent results published in Refs. [8,9] using our own data and focuses on the properties and interpretation of the Kramers-Moyal expansion terms, including the higher-order terms. We showed that the studies of Kuusela [8] and Tabar *et al.* [9] may be considered consistent with each other in spite of the fact that, in Ref. [8], 24 h recordings were analyzed while Tabar *et al.* analyzed daytime and nighttime recordings, separately. Note that both groups modeled heart rate variability using the Langevin equation assuming Gaussian noise.

Extraction of the Kramers-Moyal expansion terms requires stationarity. We compared daytime and nighttime recordings and we found that the latter are more stationary. From a physiological point of view, this is a rather obvious statement. It is interesting, however, that the effect of enhanced stationarity after detrending of the nighttime signal is obtained in the enhanced range of linearity of the $D^{(1)}$ curve and in the asymmetry of the $D^{(2)}$ curve.

The higher-order terms of the Kramers-Moyal expansion were negligible for the daytime heart rate data, while—for our data—in the nighttime fragments and for most of the 24 h data, they were not negligible (they well exceeded 10% of the first two coefficients). This effect may be related to correlations due to an oscillation in the heart rate. In the night hours, the dominant oscillation is respiratory sinus arrhythmia which leads to correlations in the signal. Due to the occurrence of higher-order coefficients in the Kramers-Moyal expansion for the nighttime and for the 24 h data, it was impossible to apply the Langevin equation to reconstruct the data. Also, in such a case, the Kramers-Moyal expansion does not reduce to the Fokker-Planck equation.

The shape of the $D^{(2)}(X)$ curve is particularly important for the interpretation of this term as due to RSA. Without detrending, we obtained an asymmetric diffusion term for only three nighttime recording fragments for the ten normals. After detrending the nighttime fragments, an asymmetry of the $D^{(2)}$ was obtained for nine of the normal subjects. We interpret this asymmetry as a consequence of the different time scales of heart rate variability during the inspiration and the expiration phases of breathing. This effect may be strongly related to the properties of respiratory sinus arrhythmia as well as to the capacity of the heart for acceleration and deceleration which are both of interest in medical diagnostics.

For the five nighttime recordings of heart rate variability obtained from hypertrophic cardiomyopathy patients, we found that the diffusion term has a weaker asymmetry or is symmetrical. This indicates a possible disruption of respiratory sinus arrhythmia in these subjects. Consequently, should the effect be confirmed on a larger group of patients, the occurrence of the asymmetry may be used for diagnostic purposes.

ACKNOWLEDGMENTS

The authors acknowledge helpful discussions with Professor K. Weron and Dr. P. Góra. The paper was supported by the Polish Ministry of Science, Grant No. 496/N-COST/2009/0.

[1] Ch. Renner, J. Peinke, and R. Friedrich, Physica A **298**, 499 (2001).
[2] M. Karth, J. Peinke, Complexity **8**, 34 (2002).
[3] G. Lim, S. Kim, E. Scalas, K. Kim, and K. Chang, Physica A **387**, 2823 (2008).
[4] R. N. Mantegna and H. E. Stanley, *An Introduction to Econophysics* (Cambridge University Press, New York, 1999).
[5] Sz. Mercik and K. Weron, Phys. Rev. E **63**, 051910 (2001).
[6] M. Ausloos, K. Ivanova, and Z. Siwy, Physica A **336**, 319 (2004).
[7] A. V. Plyukhin, Physica A **351**, 198 (2005).
[8] T. Kuusela, Phys. Rev. E **69**, 031916 (2004).
[9] M. R. R. Tabar, F. Ghasemi, J. Tabar, and R. Friedrich, Comput. Sci. Eng. **8**,54 (2006).
[10] J. Kirchner, W. Meyer, M. Elsholz, and B. Hensel, Phys. Rev. E **76**, 021110 (2007).
[11] H. Risken, *The Fokker-Planck Equation Methods of Solutions and Applications*, Springer Series in Synergetics (Springer, Berlin, 1989).
[12] N. G. van Kampen, *Stochastic Processes in Physics and Chemistry* (North-Holland, Amsterdam, 1981).
[13] R. Mannella and V. Palleschi, Phys. Rev. A **40**, 3381 (1989).

[14] P. Zarzycki, MS thesis, Warsaw University of Technology, 2003.
[15] M. Malik, J. T. Bigger, A. J. Camm, R. E. Kleiger, A. Malliani, A. J. Moss, and P. J. Schwartz, Circulation **93**, 1043 (1996).
[16] F. Beckers, D. Ramaekers, and A. E. Aubert, Cardiovasc. Eng. **1**, 77 (2001).
[17] D. Cysarz, D. von Bonin, P. Brachmann, S. Buetler, F. Edel-Hauser, K. Laederach-Hofmann, and P. Heusser, Physiol. Meas. **29**, 1281 (2008).
[18] P. Ch. Ivanov, M. G. Rosenblum, C.-K. Peng, J. E. Mietus, S. Havlin, H. E. Stanley, and A. L. Goldberger, Physica A **249**, 587 (1998).
[19] A. Bauer, J. Kantelhardt, P. Barthel, R. Schneider, T. Mäkikallio, K. Ulm, K. Hnatkova, A. Schömig, H. Huikuri, and A. Bunde, Lancet **367**, 1674 (2006).
[20] P. Grossman, F. H. Wilhelm, and M. Spoerle, Am. J. Physiol. Heart Circ. **287**, H728 (2004).
[21] F. Yasuma and J. Hayano, Chest **125**, 683 (2004).